Liquid Crystals
Publication details, including instructions for authors and subscription information:
http://www.informaworld.com/smpp/title~content=t713926090

X-ray diffraction by liquid-crystalline elastomers

C. Degert[a]; P. Davidson[b]; S. Megtert[b]; D. Petermann[b]; M. Mauzac[a]
[a] Centre de Recherche Paul Pascal, Université de Bordeaux I, Pessac, France [b] Laboratoire de Physique des Solides, associé au CNRS, Btiment 510, Université Paris XI, Orsay, France

To cite this Article Degert, C. , Davidson, P. , Megtert, S. , Petermann, D. and Mauzac, M.(1992) 'X-ray diffraction by liquid-crystalline elastomers', Liquid Crystals, 12: 5, 779 — 798
To link to this Article: DOI: 10.1080/02678299208029122
URL: http://dx.doi.org/10.1080/02678299208029122

LIQUID CRYSTALS, 1992, VOL. 12, NO. 5, 779–798

X-ray diffraction by liquid-crystalline elastomers

by C. DEGERT†, P. DAVIDSON*‡, S. MEGTERT‡,
D. PETERMANN‡ and M. MAUZAC†
†Centre de Recherche Paul Pascal, Université de Bordeaux I,
Avenue A. Schweitzer, F 33600 Pessac, France
‡ Laboratoire de Physique des Solides, associé au CNRS, Bâtiment 510,
Université Paris XI, F 91405 Orsay, France

(*Received 9 October 1991; accepted 30 April 1992*)

A new series of mesomorphic side chain polysiloxane networks has been recently synthesized in which the chemical nature of the linkage and the mesogenic group have been varied and the gelation conditions during the chemical reaction have been studied. This paper presents an X-ray diffraction study of the mesogenic group orientation in stretched samples of these networks. The angular extension of the so-called wide angle diffuse ring is used to estimate the orientational order of the mesogenic group versus strain. To perform these experiments, a special stretching device was developed and a new two-dimensional X-ray detector was used which allowed us to collect the data in a few minutes. On stretching, it was observed that the mesogenic groups orient themselves perpendicular to the stress direction for all of the samples but for one for which the parallel orientation prevailed. This prevents the establishment of a simple general law. From another point of view, the polymer concentration during the chemical reaction, which controls the gelation, is shown to be an important parameter with which to understand the physical properties: the networks synthesized below the gel point do not display reproducible and reversible behaviour, rather they flow when they are stretched. Conversely, all of the networks synthesized above the gel point really show the same well-defined behaviour independent of the sample history. Their orientational order increases regularly with the strain, first quickly, then moderately until it eventually saturates. This saturation value of the mesogenic group orientational order does not reach the nematic order parameter of the same (uncross-linked) mesomorphic side chain polymers. This suggests that the cross-links may create local tensions which disturb the nematic field.

1. Introduction

Liquid-crystalline elastomers form a new class of polymeric compounds [1] which has very interesting physical behaviour since their mechanical properties are strongly coupled to their electrical and optical ones [2]. Among others, they exhibit such unusual effects as a strong shape variation when subjected to an electric field or a strong optical birefringence when subjected to a mechanical stress. They may be produced either by cross-linking a mesomorphic polymer [1] or by direct grafting of mesogenic groups and linkages on commercial backbones [3]. Special interest has been devoted to the class of networks in which the mesogenic groups are linked as side chains via flexible spacers to the network chains. These networks are then called mesomorphic side chain networks [4]. According to the temperature, these compounds may exhibit the usual

* Author for correspondence.

0267–8292/92 $3·00

phases: isotropic liquid, nematic, smectic A, chiral smectic C, crystalline and so on. The chiral networks have been particularly studied in view of possible industrial applications [2]. As for mesomorphic side chain polymers, these networks may also exhibit a glass transition below which a mesomorphic state may be frozen.

It was soon recognized [1] that applying a mechanical stress to such a network in a mesophase tends to orient the mesogenic groups. This effect may be studied by measuring the sample birefringence versus the strain or by performing infrared spectroscopy [5] or X-ray diffraction [6] experiments on strained samples. This last technique allows us to determine the preferred direction of the mesogenic groups with respect to the stretching direction [6] because the lateral interferences between the mesogenic groups give rise to the so-called wide angle diffuse ring at $s = 1/4{\cdot}5\ \text{Å}^{-1}$ (**s** is the scattering vector, $s = (2\sin\theta)/\lambda$ where 2θ is the scattering angle and λ is the selected X-ray wavelength). A careful analysis [7–10] of this wide angle diffuse ring can also lead to a quantitative relation between the applied strain and the orientational order of the mesogenic groups. This analysis, performed on several polyacrylate networks of the same homologous series, did indeed show that orientational order of the mesogenic groups increases with the strain to reach values comparable but slightly smaller than those displayed by the mesophases of similar side chain polymers aligned in a magnetic field.

A new series of mesomorphic side chain polysiloxane networks has been recently synthesized in which the cross-linking density, the chemical nature of the linkage and the nematogenic or smectogenic character of the mesogen have been varied [3]. We describe here measurements by X-ray diffraction of the orientational order parameter versus strain for several members of this new series. We then discuss these results in relation to similar studies [5–10], to the behaviour of mesomorphic side chain polymers and also to the gelation conditions during the chemical reaction.

2. Experimental

2.1. *Materials*

All of the materials investigated belong to the same polysiloxane network series of general scheme:

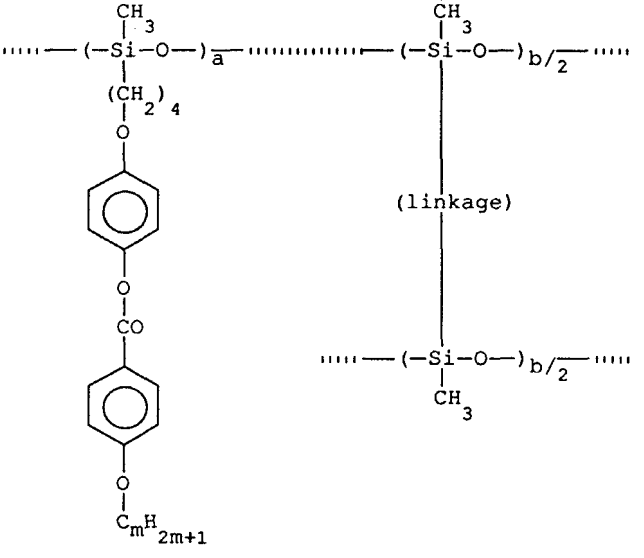

where the degree x of cross-linking is defined as:

$$x = \frac{b/2}{a + (b/2)}$$

and is equal to 10 per cent for all of the compounds studied, m is the number of methylene groups in the terminal aliphatic chain ($m = 1, 4$) and the linkage is either a flexible aliphatic chain $-(CH_2)_{10}-$ called '10' or a bifunctional mesogenic group: $-(CH_2)_4-O-\phi-OCO-\phi-O(CH_2)_4-$ called '4-4'. A given network will then be labelled R_{4m}^{linkage}, where the linkage is either 10 or 4-4. The average degree of polymerization of the initial polymethylhydrogenosiloxane chains is of 70 units. The networks were obtained by a one step hydrosilylation reaction [3] between the silane groups of the backbone and the vinyl end groups of both the mesogenic moieties and the linkages. This mesomorphic network family is derived from a series of side chain polysiloxanes already described [11]. The different samples studied and their polymorphism are shown in the table.

Actually, three different R_{41}^{10} samples have been studied; they differ only in the polymer concentration (c in millimoles of siloxane units cm^{-3} of toluene [3]) in the chemical reaction. The first R_{41}^{10} sample ($c = 1{\cdot}6\,\text{mmol}\,\text{cm}^{-3}$) simply called R_{41}^{10} in the following, was synthesized above the percolation threshold, also called the gel point, which means that the network has the same dimensions as the sample itself. The second R_{41}^{10} sample ($c = 1{\cdot}2\,\text{mmol}\,\text{cm}^{-3}$) called R_{41}^{10}(b) was synthesized just below the gel point. This means that large networks exist in this sample but none of them has the sample dimensions. The last R_{41}^{10} sample ($c = 0{\cdot}9\,\text{mmol}\,\text{cm}^{-3}$) called R_{41}^{10}(c) was synthesized well below the gel point; therefore it must only contain networks of a rather small size. The other networks R_{41}^{44}, R_{44}^{10} and R_{44}^{44} were all synthesized above the gel point and we shall, sometimes, call them, together with R_{41}^{10}, percolated networks in the following. The grafting of the mesogenic groups and the cross-linking as well, occur simultaneously in solution (concentration below $2\,\text{mmol}\,\text{cm}^{-3}$). Under these conditions, a liquid-crystalline pre-organization should be avoided.

It should also be mentioned here that none of these percolated networks could be aligned in a magnetic field of 4·7 T. This has already been reported for other kinds of side chain mesomorphic networks in the literature [10].

Samples in a roughly parallelepipedic shape were cut for the X-ray diffraction experiments. Their dimensions were: length $\approx$5–10 mm, breadth $\approx$1·5 mm and thickness $\approx$0·5–1·5 mm.

2.2. *Stretching device*

A special apparatus was built in order to stretch the networks in the different mesophases and perform *in situ* X-ray diffraction. This apparatus meets the following requirements.

(i) The sample can be stretched (manually or with a motor) to a given value λ of the strain, $\lambda = L/L_0$ where L_0 is the original length of the sample and L is its length when it is stretched.

(ii) The stretching is made symmetrically with respect to the sample centre, so that during the stretching operation, the centre of the sample probed by the X-ray beam does not move.

(iii) If necessary, the sample can be rotated around its stretching vertical axis.

R_{41}^{10}	g	9°C			S_A	50°C	N	79°C	I
R_{41}^{44}	g	13°C					N	100°C	I
R_{44}^{10}	g	13°C	C	62°C	S_A			137°C	I
R_{44}^{44}	g	14°C	C	51°C			N	127°C	I

Polymorphism of the different side chain mesomorphic networks [3].

(iv) The temperature is controlled to within ± 1°C over the whole mesomorphic range (which is more convenient than using stretched frozen samples).

(v) The device allows *in situ* X-ray diffraction.

This set-up is sketched schematically in figure 1. The sample (9) is placed vertically and held at its two extremities by two steel clamps (1) which are themselves fixed onto two mobile carriages (2). These carriages heated by resistors (5) are connected to a worm gear (7) which controls their displacement. Two other translation rods (4) ensure the mechanical stability of the device. An aluminium shield (6) equipped with thin (10 μm) mylar X-ray windows ensures the thermal insulation from the surrounding atmosphere. Finally, the whole set-up is mounted on micrometric stages for translation along the three axes and rotation around the vertical one. The sample is inserted by declutching the carriages from the worm gear and opening the clamps. The length L_0 is determined at the beginning of the experiment by measuring the distance between the clamps with a ruler. L_0 is measured with an error of at most 10 per cent and this represents the largest error in λ since the error in the clamp displacement is negligible in comparison. At this point it is checked, by X-ray diffraction, that the sample is in a macroscopically unoriented relaxed state.

2.3. *X-ray apparatus*

A rotating copper anode X-ray generator equipped with a microfocus and operated under 55 kV and 20 mA delivers the X-ray beam. This beam is monochromatized (λCu–K_α = 1·541 Å) by reflection from a vertically bent graphite slab. The X-ray source is located at the focus of the slab so that a roughly parallel beam is obtained. Several slits define the lateral beam dimensions to a square of 1 mm edge and its intensity is about 10^8 photons^{-1} at the sample level. The scattered X-rays are collected on a two-dimensional detector at a distance of 70 mm from the sample. Exposure times were typically five minutes.

The two-dimensional detector [12] which we have used is a proportional detector which means that it is able to analyse the X-ray photon energy (about 30 per cent resolution), it is made with an anode wire plane for the high voltage supply (50 wires of 20 μm diameter, 2 mm pitch) set in the middle of a 6 mm gap chamber and it uses an $ArCH_4$ gas flow at about 0·1 bar. The useful entrance window is made of a 100 × 100 mm beryllium sheet and the overall detector size is 200 × 200 mm [12]. Located on the opposite side of the beryllium window is a continuous resistive cathode plane from which the impinging events are spatially localized. For each absorbed photon in the gas, an impulse is generated at an X–Y position on the anode grid (avalanche process). By influence, this amount of charges creates in turn another amount of charge at the same position on the cathode plane. These charges move to the ground via four specially designed and located collectors through four preamplifiers. The electronic principle for localizing the X–Y position of an incoming photon is based on the analysis of the time that these charges take to travel across the cathode plane towards the

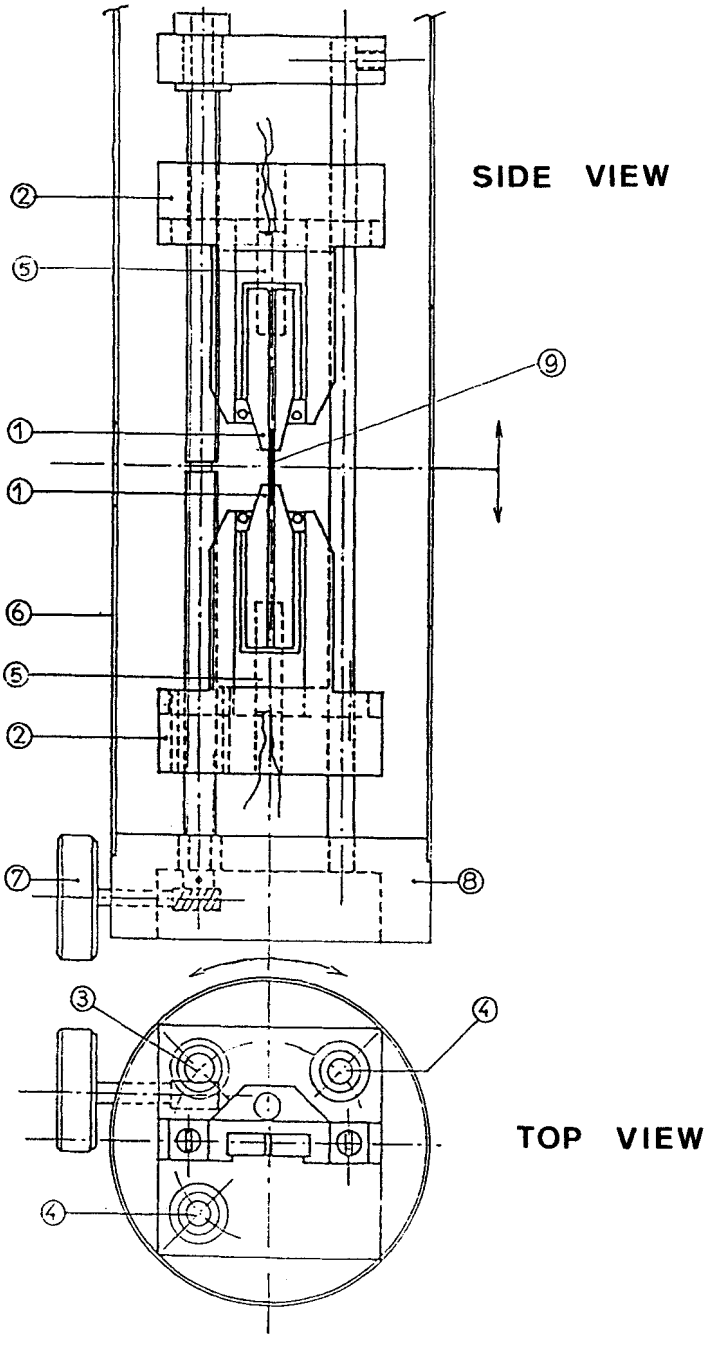

Figure 1. Stretching device: (1) steel clamps; (2) mobile carriages; (3) driving screw; (4) translation rods; (5) heating resistors; (6) aluminium shield; (7) worm gear; (8) mounting plate; (9) sample.

collectors (propagation of an impulse along a dispersive resistive-capacitive delay line). A time to digital encoder is used as the interface with the acquisition system. Under normal working conditions, the spatial resolution is about a $(0{\cdot}7\,\text{mm})^2$ square for a maximum admissible counting rate of about $10\text{–}20 \times 10^3$ counts s^{-1}. Owing to the low gas pressure and its nature, the quantum efficiency is quite low: about 15 per cent.

2.4. *Data treatment*

A typical two-dimensional recording of the X-ray scattered intensity is shown in figure 2. The wide angle diffuse ring is easily observed and its polar angular extension is the main experimental information of interest for our study. A computer program was developed to draw the curves $I(\theta)$ of the scattered intensity in the wide angle diffuse ring versus the polar angle θ with respect to the director. This curve has a maximum for $\theta = 90°$ and minima for $\theta = 0°$ and 180°. This program computes the function $I(\theta)$ along a half circle (of 13 pixels thickness) centred on the beam stop and going through the wide angle diffuse ring by averaging 13 pixels at the same angle θ (see figure 3). This curve has in its two wings or at its centre several rapid oscillations. These oscillations come from a small spatial inhomogeneity due to the multiwire structure of the two

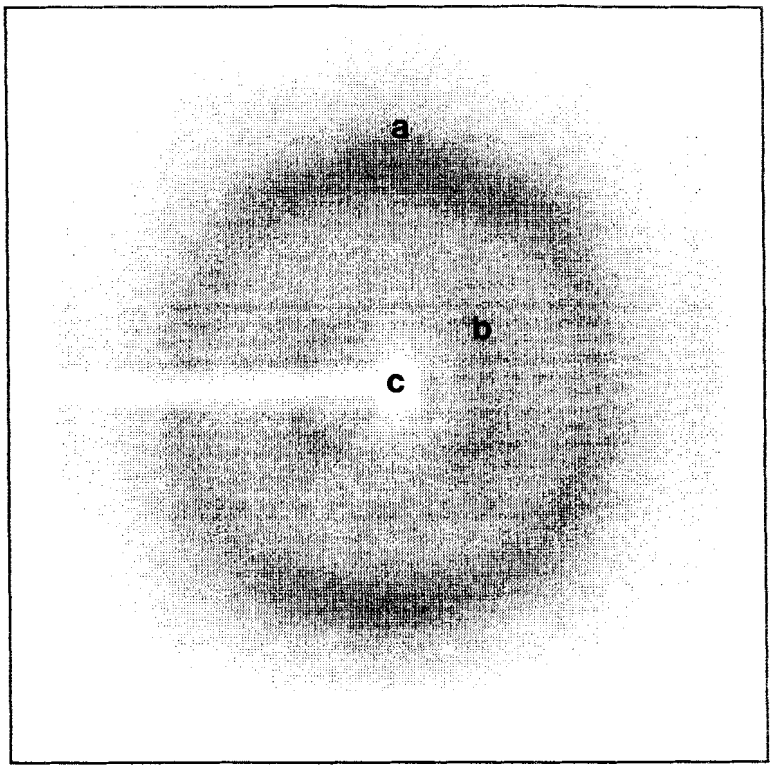

Figure 2. Typical two-dimensional recording of the X-rays scattered by a mesomorphic side chain network sample (R^{44}_{44}, $\lambda = 2{\cdot}4$, 50°C). (*a*) Partially oriented wide angle diffuse ring; (*b*) intramolecular longitudinal interferences probably involving the silicon atoms of the network chains; (*c*) beam stop. Each point symbolizes an image pixel the grey level of which represents the number of photons detected. The blurred horizontal lines arise from a small detector counting inhomogeneity due to its multiwire structure.

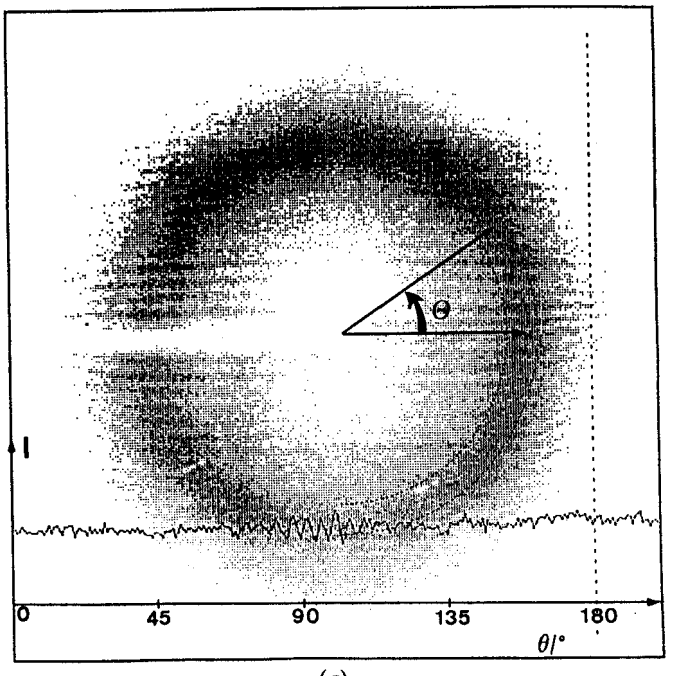

(a)

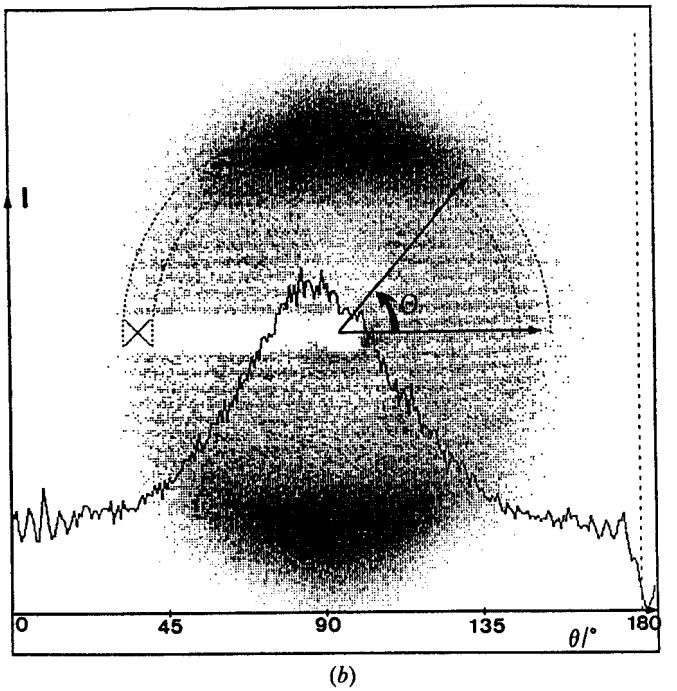

(b)

Figure 3. Two dimensional images obtained with a (*a*) completely isotropic sample (R_{41}^{44}, $\lambda = 1$, room temperature); (*b*) highly oriented sample (R_{41}^{10}(c), $\lambda = 4$, room temperature). Superimposed on the images are the thick half circle used to average the intensity in the wide angle, diffuse ring at constant polar angle θ and the $I(\theta)$ function (in arbitrary units) used to obtain $\Delta\theta^{1/2}$, a measure of the orientational order of the sample. (The small oscillations in the wings (*b*) and at the centre (*a*) of the $I(\theta)$ function are due to the detector multiwire structure.)

dimensional detector. These oscillations can be corrected either by dividing the image by that of a flat background or in a simpler but less accurate way, by considering the oscillations' midpoints. The Lorentz polarization corrections were found to be negligible for these scattering angles and geometry. The whole procedure adopted to obtain the function $I(\theta)$ has been defined once and for all and was used in exactly the same way during all of the experiments.

The problem now is to relate the curve $I(\theta)$ with an orientational order parameter that would characterize the quality of the orientational order of the sample. Here the following point should be carefully acknowledged: let us consider for instance a mesomorphic network in the smectic A phase (the same would hold true for a nematic phase of a smectic C phase as well). In the absence of strain ($\lambda = 1$), the distribution of the smectic domains inside the sample is isotropic; the sample texture is that of a perfect smectic powder as can be checked by the appearance of a uniform small angle, powder sharp ring due to the reflection of X-rays by the smectic layers. Each smectic domain has a nematic order parameter S described, for instance, by the Maier–Saupe theory [13] but S cannot be directly measured with X-rays because of the powder averaging. Applying a mechanical stress to the network has as a first step essentially the effect of breaking the isotropy of the smectic domain powder distribution rather than increasing S inside each domain. As a second step, when all of the domains are aligned in the same direction which can be checked by the fact that the small angle, sharp ring has condensed into two Bragg spots, it is quite possible that increasing the stress even more could also influence the nematic order parameter. Thus it appears that the function $I(\theta)$ is related to a complex combination of both the sample mosaicity and the nematic order parameter. Therefore the classical treatment [14, 15], used in the case of monodomains, of this function to obtain S cannot be applied here. This situation was soon recognized and another type of data treatment [7–10] has been used: this treatment assumes that the function $I(\theta)$ can be represented by the convolution of an orientational distribution function with the scattering function of a perfectly aligned sample with the side chains in their most probable conformation. Though this type of data treatment is presently the most realistic one, it has the drawbacks of needing a rather heavy computational procedure and of depending upon the side chain conformation which seems to fit the data best. Anyway, this kind of treatment also leads to an orientational order parameter which represents the side chain orientational order averaged not only within a given smectic domain (i.e. the nematic order parameter) but also by the powder domain distribution. For convenience, we decided therefore, to address this problem by only considering the full width at half maximum of the $I(\theta)$ function. This value, called in the following $\Delta\theta^{1/2}$, decreases regularly when the orientational order increases. It naturally takes into account both types of averages (nematic and powder-like) and thus characterizes the overall alignment of the side chains which is the quantity of interest for possible applications. The statistical error introduced (especially in the oscillation smoothing operation) by our global data treatment has been estimated to be about 10 per cent. For information, we also present our results in the more usual way of plotting the inverse of $\Delta\theta^{1/2}$ versus strain. This procedure indeed provides an estimate of the nematic order parameters for low molecular weight mesogens within an error of at most 10 per cent [16]. Here for the reasons just mentioned, it will only give an estimate of an orientational order parameter which we shall call P_2 (more precisely $P_2 = 14{\cdot}5/\Delta\theta^{1/2}$ when $\Delta\theta^{1/2}$ is expressed in degrees, the numerical value 14·5 is drawn from various examples in the literature [7, 14–16]) according to the notation of Mitchell *et al.* [7]. Here, this orientational

order parameter is defined with respect to the liquid crystal director so that it is always positive whatever the orientation direction, parallel or perpendicular to the deformation axis.

3. Results

In this section, we present the $\Delta\theta^{1/2}$ and P_2 curves versus the strain λ for the different samples studied. However, let us first mention a few observations. Samples not submitted to any stress do indeed give rise to an isotropic diffuse scattering (see figure 3(*a*)). We did not observe any spontaneous alignment due to the sample surfaces though surface effects can conceivably exist and have been reported sometimes [5, 6]. On stretching, the mesogenic groups aligned themselves in the direction perpendicular to that of the stretch (see figures 2 and 3(*b*)). This was observed for all of the samples except for the R_{41}^{44} network for which the parallel direction prevailed. Furthermore, whatever the orientation of the mesogenic group with respect to the stretching direction, the opposite orientation was systematically observed upon compression. This fact has already been reported [4]. Biaxiality was sometimes reported [5, 6] when the side chains aligned perpendicular to the deformation axis. We did not detect any such effect though we did not specifically look for it.

The sample's homogeneity was checked systematically by translation in the X-ray beam. All of the samples presented in this paper were found to be fairly homogeneous. Within the experimental accuracy (10 per cent on both λ and $\Delta\theta^{1/2}$), the results and behaviour are reproducible among different samples of the same network. Moreover, still within the experimental accuracy, samples cross-linked above the gel point during the chemical reaction (and only these percolated network samples) show a truly reversible and reproducible behaviour. In this case, relaxation starts as soon as the stress is suppressed and is completed within $\frac{1}{2}$–2 h depending on the sample and the maximum strain achieved and then no time dependence could be detected on a time scale ranging from 2 h to several days. On the macroscopic scale, we observe the healing of sample buckling within about an hour [6]. On the contrary, samples synthesized below the gel point namely R_{41}^{10}(b) and R_{41}^{10}(c) do not display a reversible behaviour. These samples do not present a percolated network and can then undergo a drastic flow of the polymer chains. For instance, sample R_{41}^{10}(b) finally reaches an isotropic state but keeps a small (10–20 per cent) permanent strain when the stress is removed. Sample R_{41}^{10}(c) synthesized well below the gel point does not relax even after several days, its length never returns to L_0 and it will hardly disorient.

Figures 4–10 shows the behaviour of the full width at half maximum $\Delta\theta^{1/2}$ of the $I(\theta)$ function and that of P_2 versus strain for the different samples studied. Except for R_{41}^{10}(b) and R_{41}^{10}(c), these plots include measurements recorded indifferently on increasing and decreasing strains or on successive stretches with relaxations ($\lambda = 1$) in between or also using different mechanical histories. Such a method of obtaining the results does not markedly increase the dispersion of the measurements (due to the experimental errors) which demonstrates the reversibility and reproducibility within 10 per cent, of the phenomenon for all of the infinite network samples.

Strain values of about 2 and exceptionally 5 were reached. For sample R_{41}^{10}(b) a compression curve ($\Delta\theta^{1/2}$ versus λ for $\lambda < 1$) has also been recorded down to $\lambda \approx 0{\cdot}6$ and is shown in figure 5. It seems that compression induces more or less the same orientational order as stretching.

The samples were studied at only one temperature, either room temperature of just above the C–S_A transition temperature for R_{44}^{10} and R_{44}^{44}. R_{41}^{10} was the only sample to be

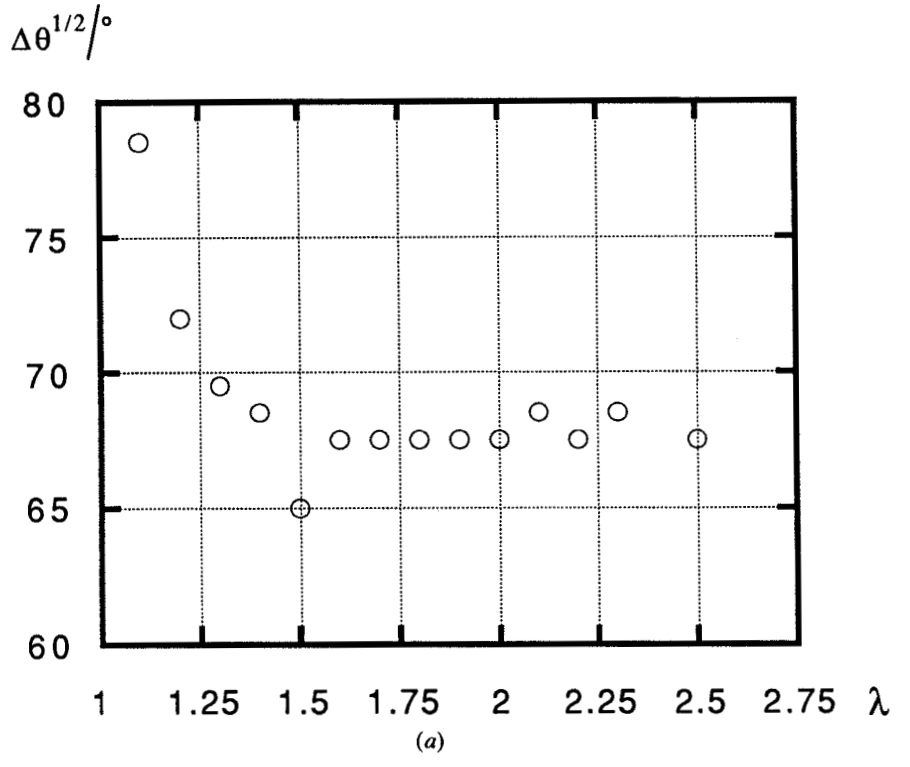

(*a*)

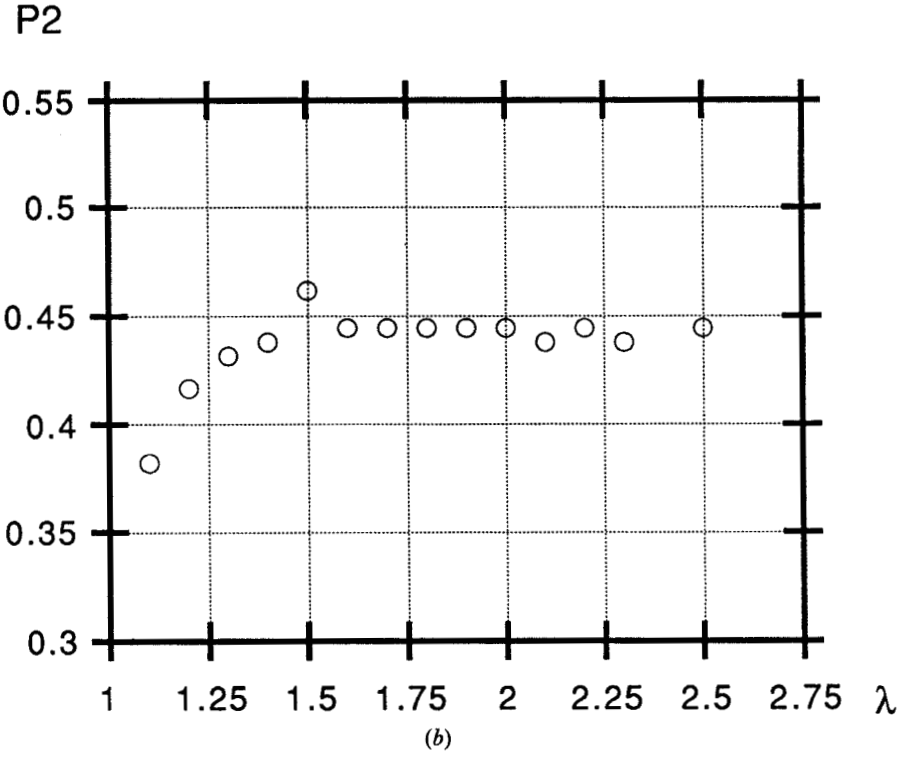

(*b*)

Figure 4. $\Delta\theta^{1/2}$ (*a*) and P_2 (*b*) versus λ for sample R_{41}^{10} in the S_A phase at room temperature.

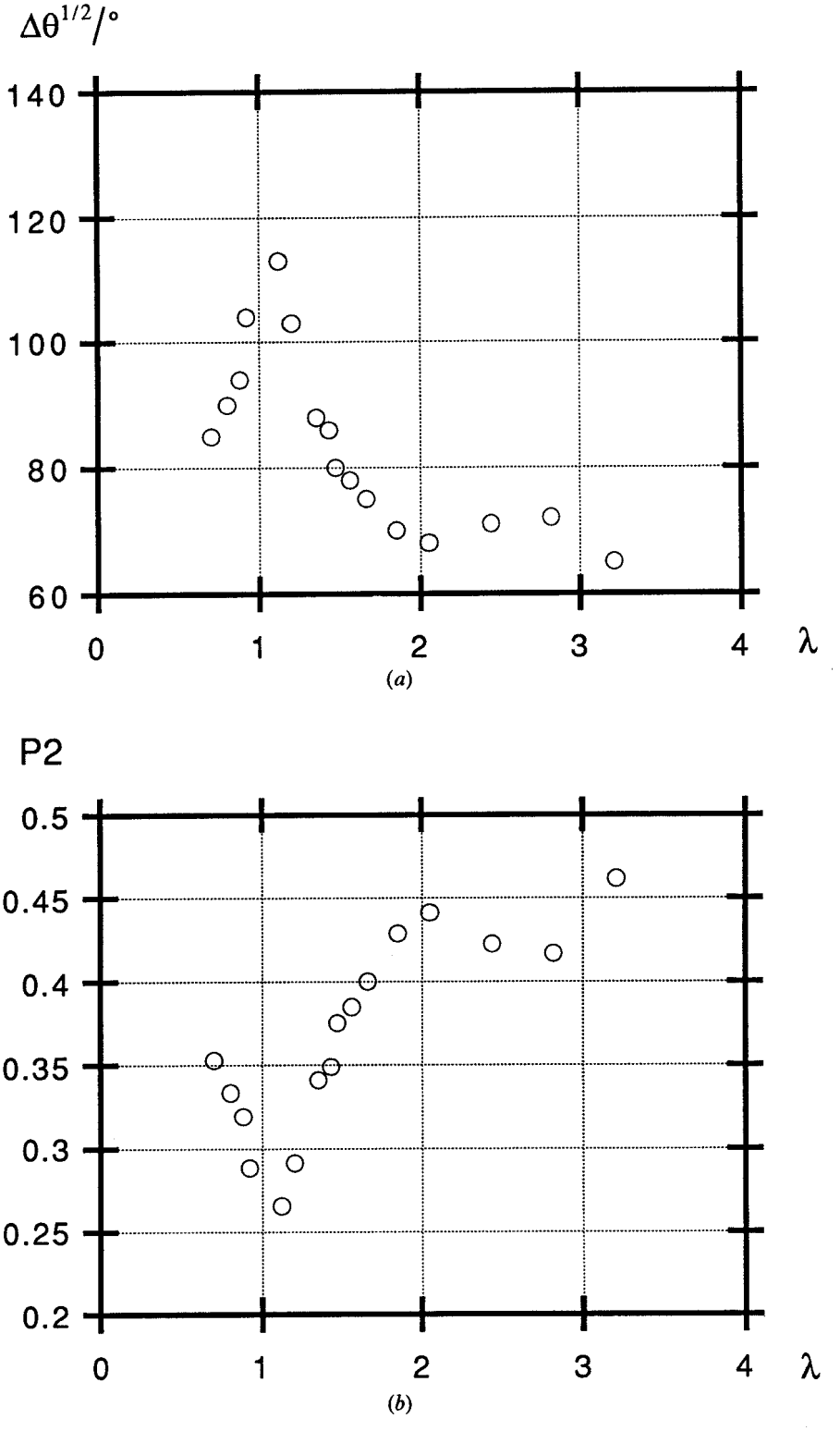

Figure 5. $\Delta\theta^{1/2}$ (*a*) and P_2 (*b*) versus λ for sample R_{41}^{10}(b) in the S_A phase at room temperature.

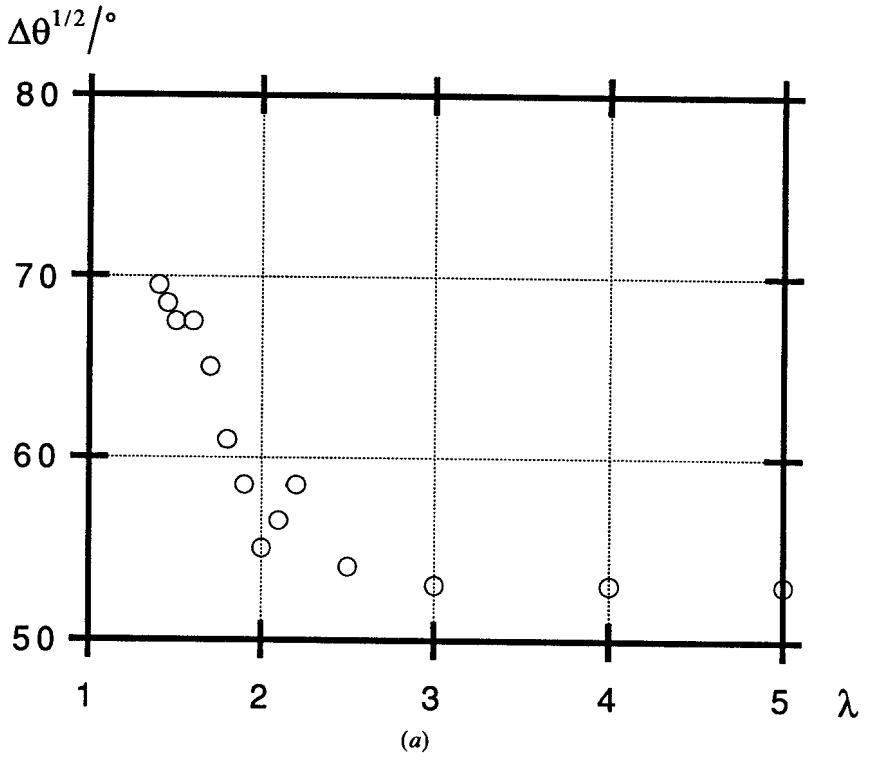

(*a*)

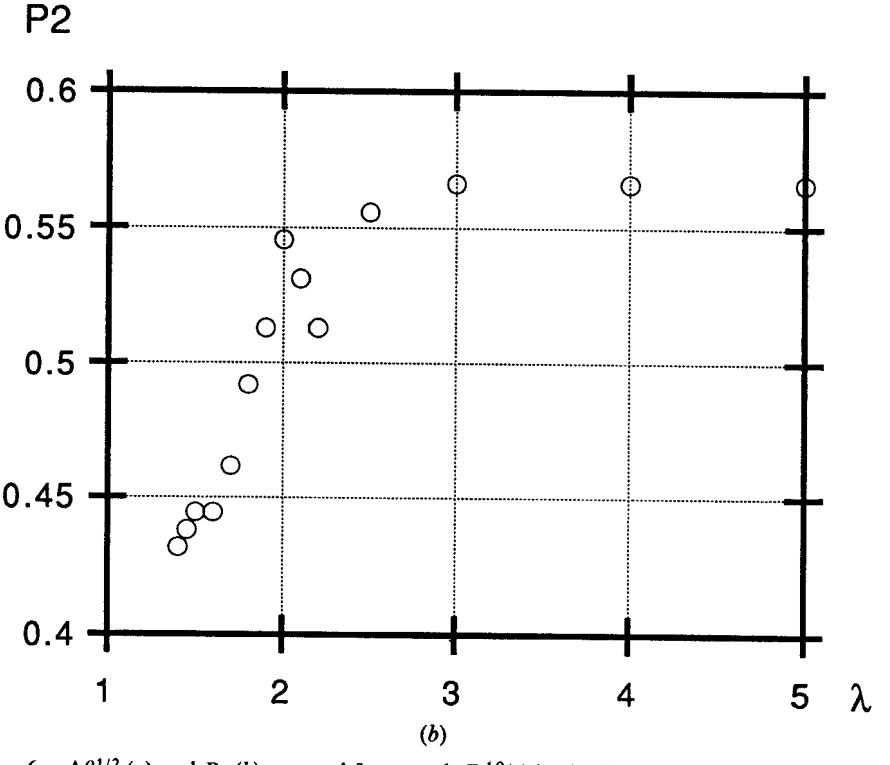

(*b*)

Figure 6. $\Delta\theta^{1/2}$ (*a*) and P_2 (*b*) versus λ for sample R_{41}^{10}(c) in the S_A phase at room temperature.

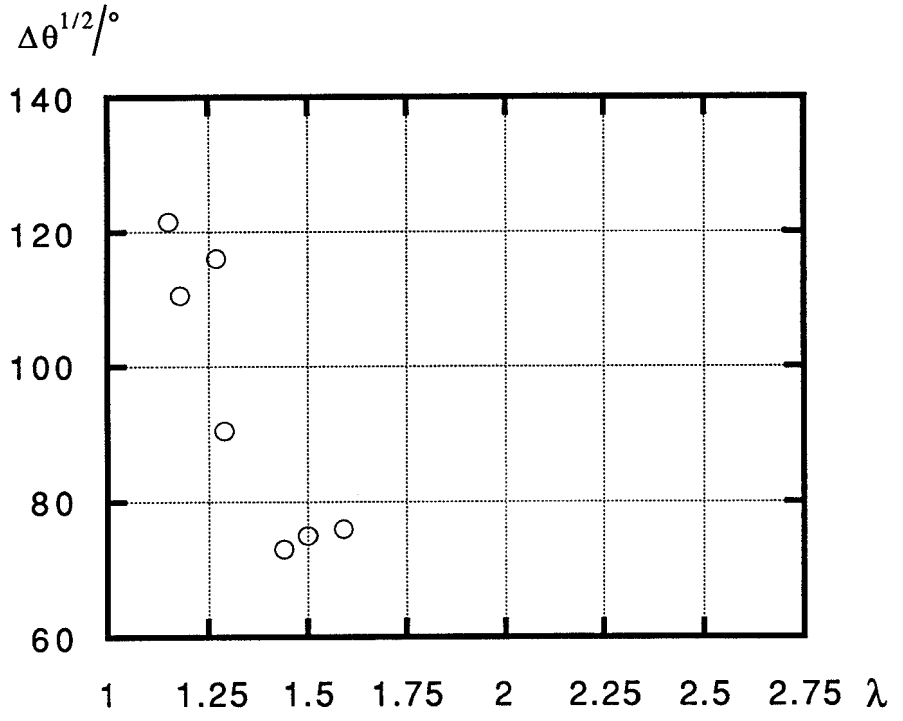

(*a*)

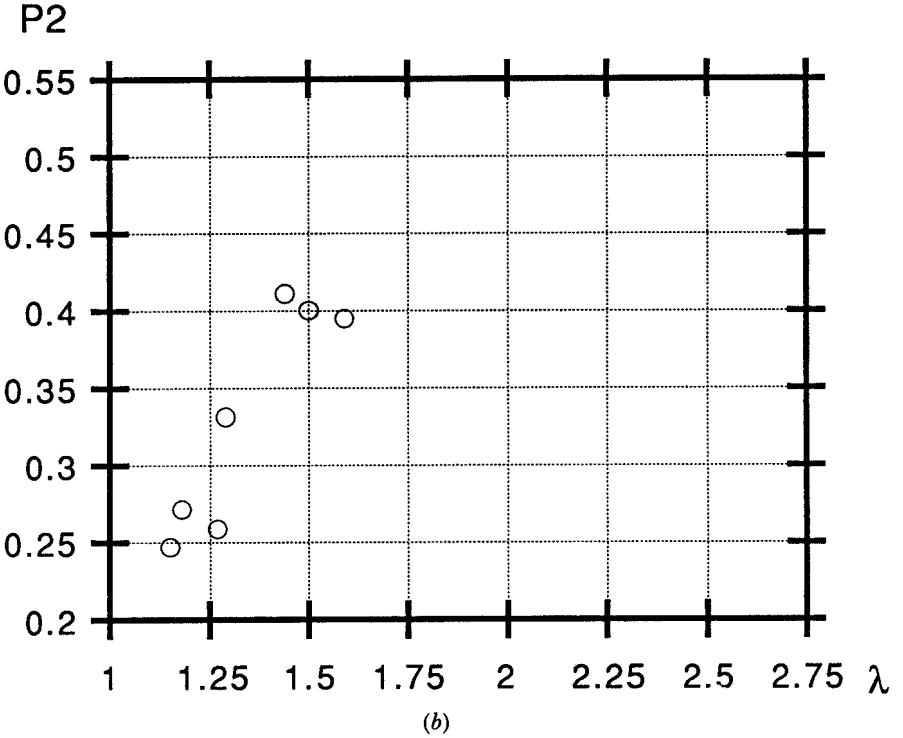

(*b*)

Figure 7. $\Delta\theta^{1/2}$ (*a*) and P_2 (*b*) versus λ for sample R_{41}^{10} in the N phase at 60°C.

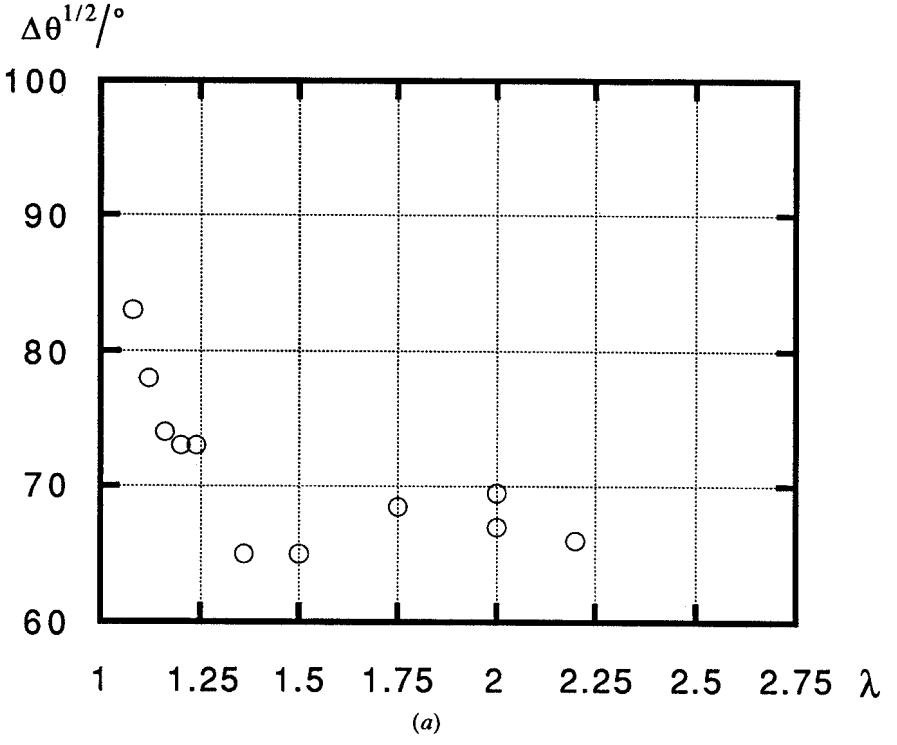

(*a*)

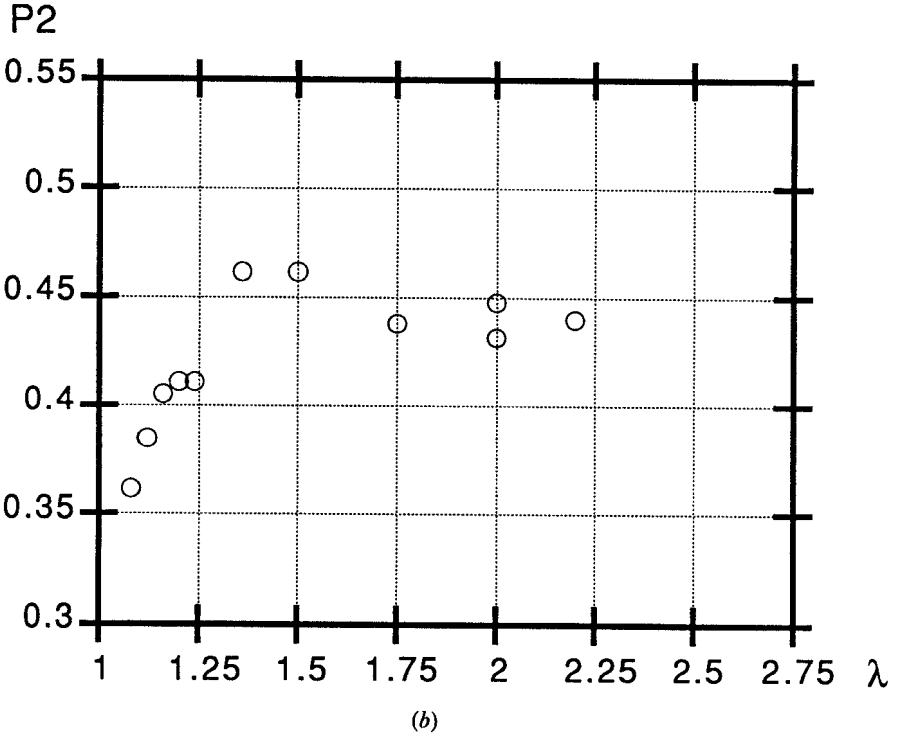

(*b*)

Figure 8. $\Delta\theta^{1/2}$ (*a*) and P_2 (*b*) versus λ for sample R_{41}^{44} in the N phase at room temperature.

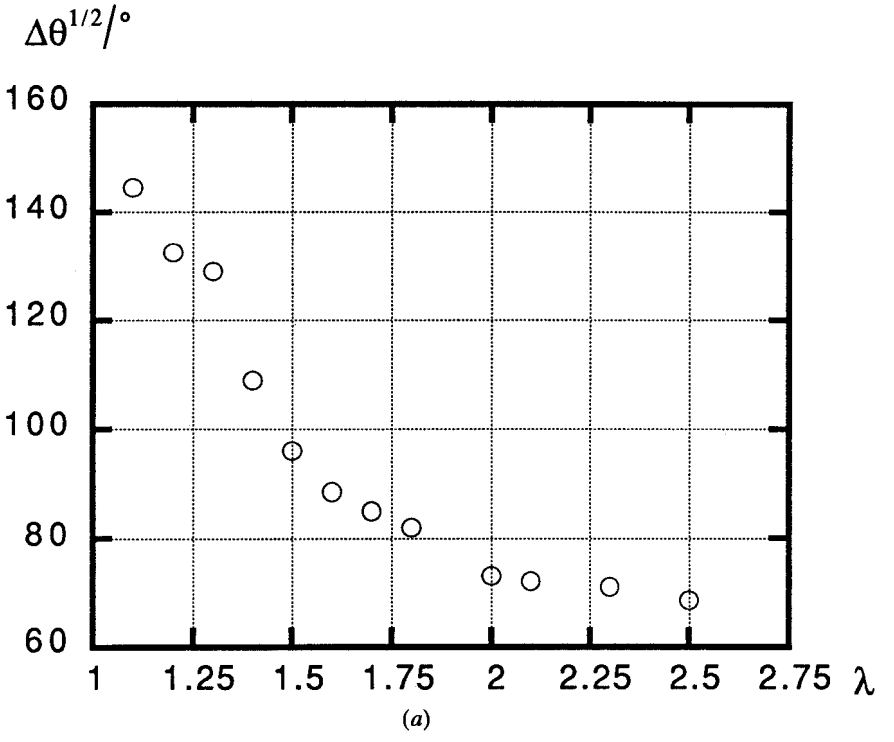

(a)

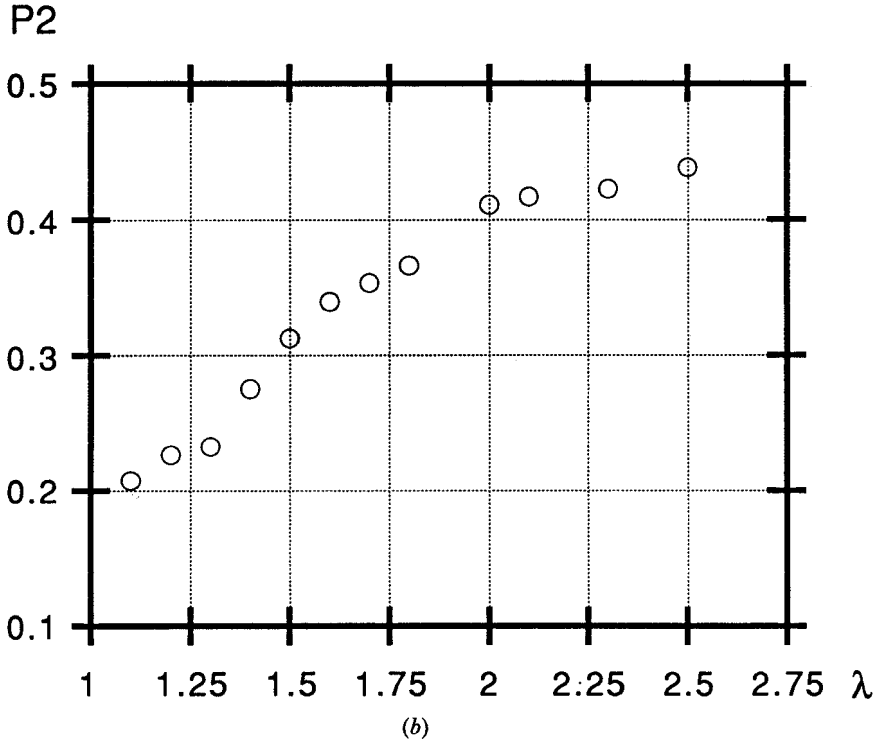

(b)

Figure 9. $\Delta\theta^{1/2}$ (*a*) and P_2 (*b*) versus λ for sample R_{44}^{10} in the S_A phase at 65°C.

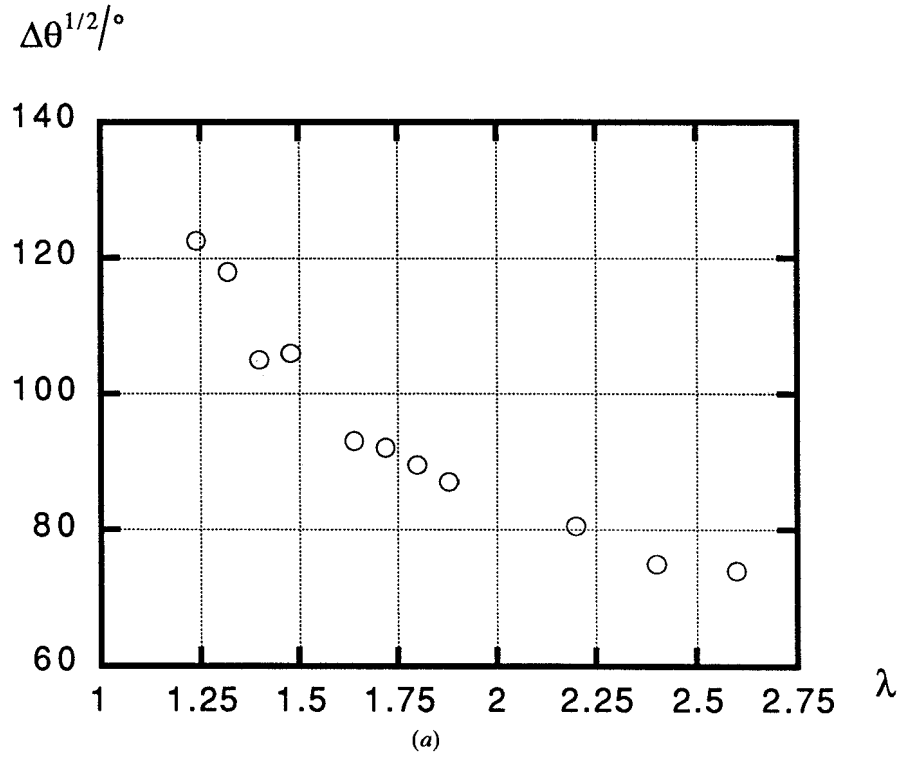

(*a*)

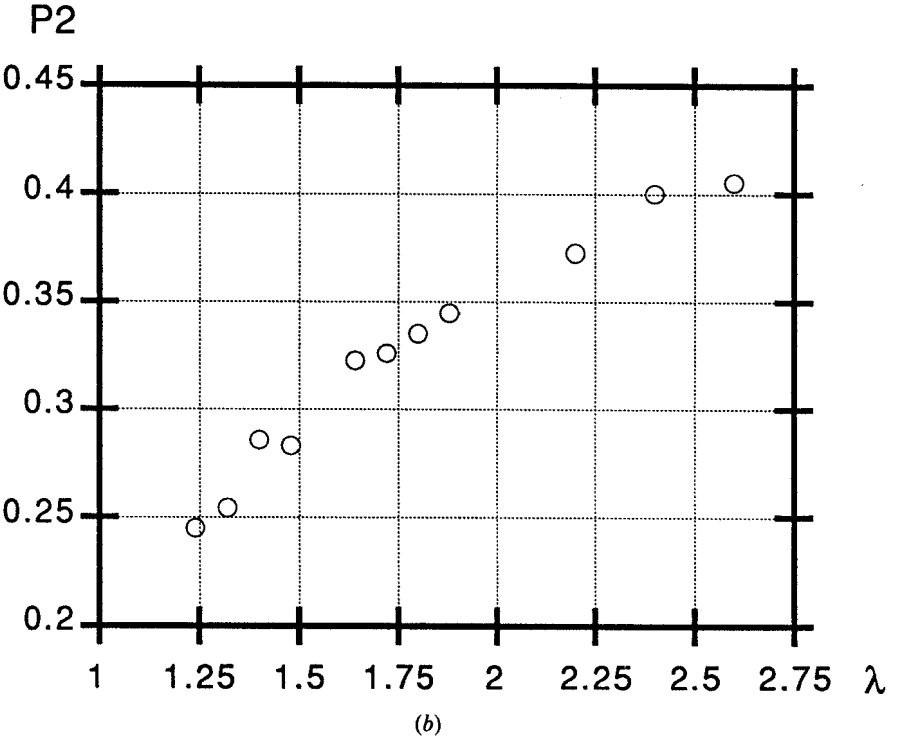

(*b*)

Figure 10. $\Delta\theta^{1/2}$ (*a*) and P_2 (*b*) versus λ for sample R_{44}^{44} in the N phase at 60°C.

probed both at room temperature and around 60°C in order to compare its behaviour in the N and S_A phases.

All of the stretching curves (see figures 4–10) are rather similar. $\Delta\theta^{1/2}$ regularly decreases with strain, quickly at the beginning, moderately for large λ values and sometimes it even saturates at some constant value. Of course, the P_2 curves behave in the opposite way. Even small strain values ($\lambda \approx 1{\cdot}2$) already induce a quite appreciable global orientational order ($\Delta\theta^{1/2} = 50°$, $P_2 \approx 0{\cdot}3$) [5, 7].

4. Discussion

We comment first on the relative orientational order of the mesogenic groups with respect to the stretching direction in the side chain elastomers. This question is a complicated one since opposite behaviour may be found (see [4] and references therein). Actually, it is already quite difficult to predict the relative orientation of the side chains and the backbones in the case of uncross-linked mesomorphic side chain polymers either in frozen nematic fibres [17] or in magnetically aligned nematic phases [10, 18]. Actually, if the spacers are long enough, it is assumed [10, 18] that the mesogenic groups tend to orient themselves perpendicular to the backbones in smectic A or nematic phases which display strong smectic fluctuations whereas they tend to orient parallel to the backbones in nematic phases devoid of smectic fluctuations.

From another point of view, when a classical network is uniaxially stretched, the stress essentially modifies (in a more or less affine way) the cross-links distribution [19] but there also exists some kind of nematic-like interactions [20] among the network chains. In such a case of a classical network, both phenomena have the same effect namely a slight extension of the network chains along the stretching direction. For a mesomorphic network, the nematic interactions are now mainly due to the side chains and may be rather strong. If the linkages are not mesogenic, we may assume, just like the usual networks, that the network chains are elongated along the stretching direction because of the deformation of the cross-link distribution. Therefore, by analogy with the behaviour of mesomorphic side chain polymers, we should also expect a perpendicular orientation of the mesogenic groups for all S_A phases and for the N phases which exhibit smectic fluctuations too. We should expect a parallel orientation for the mesogenic groups in the N phases which do not exhibit any smectic fluctuations. When the linkages themselves are mesogenic, the situation becomes even more complicated because the stress could align these mesogenic linkages in its direction and perhaps the whole nematic field too in a uniform way whatever the relative natural orientation of the side chains and backbones.

In the present network series, we have observed a perpendicular orientation of the mesogenic groups with respect to the stretching direction for all of the samples in the nematic and smectic A phases (These nematic phases may exhibit S_A fluctuations like that of the corresponding uncross-linked polymers [11]) except for the R_{41}^{44} network which shows the parallel orientation. If we compare this last network and the R_{41}^{10} network both in their nematic phase, we notice that replacing the aliphatic linkage by a mesomorphic (and also much more rigid) one is indeed enough to change the orientational behaviour. However, this is not the only relevant parameter since R_{44}^{10} and R_{44}^{44} orient in the same way. In front of such a complicated situation, no general rule could be obtained and therefore we shall not discuss this point any further.

The polymer concentration during the chemical reaction seems to be a crucial parameter since only the samples obtained above (or around) the gel point show

reproducible results and reversible behaviour. Let us consider the case of sample R_{41}^{10}(c) synthesized well below the gel point. First, we notice that is can be stretched to a much greater extent ($\lambda \approx 5$) than the infinite network samples which usually break before such strain values are achieved. Secondly, it is better oriented than the other samples for the same strain values ($\lambda \approx 2 \Rightarrow \Delta\theta^{1/2} \approx 60°$ for R_{441}^{10}(c) whereas $\lambda \approx 2 \Rightarrow \Delta\theta^{1/2} \approx 70°$ for the other samples). For very large strains ($\lambda \approx 3$–5), the orientational order parameter P_2 saturates at about 0·6 which is a typical value of the order parameter of (uncross-linked) polymer $P_{4,1}$ [21]. This means that the smectic domains are all oriented perpendicular to the stress direction so that the direct evaluation of the nematic order parameter is made possible. Indeed the small angle, sharp ring has then condensed into two Bragg spots. In some way, we can consider that the R_{41}^{10}(c) sample rather flows under the influence of stress so that its stretching is comparable to a fibre drawing process.

Conversely, the R_{41}^{10} sample synthesized above the gel point reaches saturation for a P_2 value of about 0·45. This value is comparable to that found in the literature for very different mesomorphic networks [7, 9]. Further stretching will not improve the order of the mesogenic groups but will only result in tearing the sample. This rather low P_2 value shows that the smectic domains cannot all be aligned perpendicular to the stress direction. It seems that the existence of a percolated network induces additional local constraints which prevent the complete ordering of the domains. This observation is consistent with the fact that side chain mesomorphic networks cannot be aligned in a magnetic field. The borderline R_{41}^{10}(b) sample synthesized just below the gel point displays a behaviour in between those of R_{41}^{10} and R_{41}^{10}(c). It is somewhat reproducible and its orientational order parameter P_2 also saturates around 0·45 though it flows slightly during stretching although larger strain values ($\lambda \approx 3$) may be obtained before sample tearing. This intermediate behaviour may reflect the influence of physical entanglements which may physically connect large but not percolated networks to build one which would have the sample dimensions.

We now discuss the influence of both the chemical formula and the mesophase type on the mechanical orientation of the percolated network samples. Actually, all these samples display roughly the same saturation values ($\Delta\theta^{1/2} \approx 65$–$70°$, $P_2 \approx 0{\cdot}40$–$0{\cdot}45$) whatever the aliphatic end chain length $m = 1$ or 4, the linkage 10 or 4-4 and even the mesophase type N or S_A. However, saturation is reached for lower strain values in the case of short end chains ($m = 1$, $\lambda \approx 1{\cdot}5$) than in the case of long end chains ($m = 4$, $\lambda = 2{\cdot}5$) irrespective of the mesophase and linkage types. At this point, it should be recalled that the experiments made with the $m = 4$ networks were carried out at higher temperatures (50–60°C) than the others. The same temperature influence may also be suspected when comparing the behaviour of R_{41}^{10} in the S_A and N phases: before saturation, for a given strain value, the orientational order is higher in the S_A phase in the N at 60°C. The saturation values reached in both phases are about the same, though.

5. Conclusion

The use of an *in situ* stretching device together with a two dimensional X-ray detector allows the quick recording of the X-ray diffraction patterns of uniaxially stretched mesomorphic networks. Our simple data treatment yields semiquantitative values of the orientational order of the mesogenic groups. This order represents an average of that of the mesogenic group both within the mesophase domains namely the nematic order parameter, and among the mesophase domains namely the mosaicity. We have shown that the polymer concentration during the chemical reaction is an

important parameter which should be taken into account in order to obtain percolated mesomorphic networks of dimensions equal to that of the sample. The influence of this parameter may explain why the behaviour of some mesomorphic networks was found to be reversible [5, 7] whereas that of others was not [22, 23]. (However, some more subtle and strange history effects have recently been demonstrated [5] even in percolated networks.) The relative order of the side chains and backbones in stretched samples is not fully understood so far and further experiments are needed to elucidate this point. All of the samples synthesized above the gel point display the same kind of behaviour: their orientational order increases with the strain first quickly, then more moderately until it eventually saturates. This saturation value is somewhat smaller than the nematic order parameter usually measured in mesomorphic side chain polymers. This suggests that, at saturation, most of the domains are oriented in the same way except a small fraction of them which are too much affected by the cross-links to orient under the stress influence. Naturally, this fraction must depend upon the cross-linking density. The same orientational order versus strain behaviour was observed whatever the nature of the mesophase, that of the linkage and that of the mesogenic group within the homologous series presented here. The only differences detected seemed to be that for a given strain the orientational order achieved depended on temperature. Most of these results are similar to those already reported [7–10] for a very different homologous series of side chain mesomorphic networks and we may wonder whether they are valid for this whole new class of compounds. Since the behaviour of all of the mesomorphic percolated networks studied seemed to be alike, one of them should be selected to study systematically the influences of the cross-linking density and that of temperature within in each mesophase. More sophisticated and accurate X-ray diffraction experiments are also under way to provide a more detailed description of the ordering process.

The authors are deeply indebted to L. Deschamps for technical assistance and for the development of the stretching device which made possible the *in situ* X-ray diffraction experiments. The authors also acknowledge very helpful discussions with B. Deloche, A. M. Levelut and R. Zentel.

References

[1] FINKELMANN, H., KOCH, H. J., and REHAGE, G. 1981, *Makromolek. Chem. rap. Commun.*, **2**, 317.
[2] ZENTEL, R., 1989, *Adv. Mat. Angew. Chem.*, **28**, 1407.
[3] DEGERT, C., RICHARD, H., and MAUZAC, M., 1992, *Molec. Crystals liq. Crystals*, **214**, 179.
[4] GLEIM, W., and FINKELMANN, H., 1989, *Side Chain Liquid Crystal Polymers*, edited by C. B. MacArdle (Blackie, Glasgow), Chap, 10, and references therein.
[5] BRÄUCHLER, M., BOEFFEL, C., and SPIESS, H. W., 1991, *Makromolek. Chem.*, **192**, 1153.
[6] FINKELMANN, H., KOCH, H. J., GLEIM, W., and REHAGE, G., 1984, *Makromolek. Chem. rap. Commun.*, **5**, 287.
[7] MITCHELL, G. R., DAVIS, F. J., and ASHMAN, A., 1987, *Polymer*, **28**, 639.
[8] DAVIS, F. J., and MITCHELL, G. R., 1987, *Polymer Commun.*, **28**, 8.
[9] BARNES, N. R., DAVIS, F. J., and MITCHELL, G. R., 1989, *Molec. Crystals liq. Crystals*, **168**, 13.
[10] MITCHELL, G. R., DAVIS, F. J., GUO, W., and CYWINSKI, R., 1991, *Polymer*, **32**, 1347.
[11] MAUZAC, M., HARDOUIN, F., RICHARD, H., ACHARD, M. F., SIGAUD, G., and GASPAROUX, H., 1986, *Eur. Polymer J.*, **22**, 137.
[12] LEMONNIER, M., PETERMANN, D., and MEGTERT, S., 1982, CNRS patent 8203344 France.
[13] DE GENNES, P. G., 1974, *The Physics of Liquid Crystals* (Clarendon Press).

[14] DELORD, P., and FALGUEIRETTES, J., 1965, *C. r. hebd. Séanc. Acad. Sci., Paris*, **260**, 2468.
[15] LEADBETTER, A. J., and WRIGHTON, P. G., 1979, *J. Phys., Paris*, **40**, C3-234.
[16] DE VRIES, A., 1972, *J. chem. Phys.*, **56**, 4489.
[17] GUO, W., DAVIS, F. J., and MITCHELL, G. R., 1991, *Polymer Commun.*, **32**, 268.
[18] DAVIDSON, P., NOIREZ, L., COTTON, J. P., and KELLER, P., 1991, *Liq. Crystals*, **10**, 111.
[19] FLORY, P. J., 1953, *Principles of Polymer Chemistry* (Cornell University Press).
[20] DELOCHE, B., DUBAULT, A., HERZ, J., and LAPP, A., 1986, *Europhysics Lett.*, **1**, 629.
[21] OULYADI, H., LAUPRÊTRE, F., MONNERIE, L., MAUZAC, M., RICHARD, H., and GASPAROUX, H., 1990, *Macromolecules*, **23**, 1965.
[22] TALROZE, R. V., GUBINA, T. I., SHIBAEV, V. P., PLATÉ, N. A., DAKIN, V. I., SHMAKOVA, N. A., and SUKHOV, F. F., 1990, *Makromolek. Chem. rap. Commun.*, **11**, 67.
[23] DAVIDOV, D. (private communication).